Abstract for the 30th Intl Workshop on Water Waves and Floating Bodies, Bristol (UK), April 12–15, 2015

Numerical Simulation of Breaking Wave Impact on a Vertical Wall

Feng Gao, Jun Zang, Chris Blenkinsopp

Department of Architecture and Civil Engineering, University of Bath
Bath, United Kingdom
E-mail: f.gao@bath.ac.uk

Highlights:

- A compressible multiphase flow solver based on OpenFOAM has been successfully applied to simulate breaking wave impact on a vertical wall.
- Different types of wave impact on a vertical wall have been produced. The results of the pressure distribution near the impact area and the maximum impact pressure have been analysed.

1. Introduction

The loading caused by steep storm waves impacting coastal and offshore structures such as vertical sea walls, FPSOs and LNG carriers can cause significant damage. Accurate prediction of the breaking wave impact pressure is a key factor in the design of such structures. The fundamental role of the extreme impact pressures that are impulsively exerted on sea walls has been underlined by both experimental (e.g. Hattori *et al.* [1]; Bullock *et al.* [2]) and theoretical (e.g. Peregrine [3]) studies. In addition, numerous numerical works have been carried out to provide a reliable tool for the estimation of wave impact pressure. Lin and Liu [4] gave an overview and discussion of the different numerical techniques which have been used for interface tracking in breaking wave simulation, while Christensen *et al.* [5] undertook a comprehensive review of advances in numerical modelling and measurement techniques for the study of the surf zone.

In this study, a compressible multiphase flow solver based on the frame of open source CFD tool – OpenFOAM is used to simulate the breaking wave propagation, overturning and impact on a vertical wall. With a suitable predefined initial condition, different types of wave impact on a vertical wall have been produced. The results of the pressure distribution near the impact area and the maximum impact pressure will be analysed.

2. Numerical tools

OpenFOAM is a freely available set of applications developed to solve particular problems in continuum mechanics, which consists of a wide range of solvers and libraries. It has gained popularity in coastal and offshore engineering studies (Jacobsen *et al.* [6]; Chen *et al.* [7]; Morgan *et al.* [8]). *twoPhaseEulerFoam* is one of the component solvers included in the OpenFOAM package. In this solver, both air and water-air mixture are treated as compressible fluids, which are continuum and described by Eulerian conservation equations. The averaged inter-phase momentum transfer term accounts for the transfer of momentum between the two phases.

The averaged momentum and continuity equations for each phase φ can be written as:

$$\frac{\partial \alpha_\varphi \overline{U}_\varphi}{\partial t} + \nabla \cdot \left(\alpha_\varphi \overline{U}_\varphi \overline{U}_\varphi\right) + \nabla \cdot \left(\alpha_\varphi \overline{R}_\varphi^{eff}\right) = -\frac{\alpha_\varphi}{\rho_\varphi} \nabla \overline{p} + \alpha_\varphi g + \frac{\overline{M}_\varphi}{\rho_\varphi} \tag{1}$$

$$\frac{\partial \alpha_\varphi}{\partial t} + \nabla \cdot \left(\overline{U}_\varphi \alpha_\varphi\right) = \Gamma_\varphi \tag{2}$$

where the subscript φ denotes the phase, α is the phase fraction, $\overline{U}_\varphi$ is the averaged phase velocity, $\overline{R}_\varphi^{eff}$ is the combined Reynolds and viscous stress, $\overline{M}_\varphi$ is the averaged inter-phase momentum transfer term and Γ_φ stands for the mass gained by each phase per unit volume and time.

Combining equation (2) for the two phases when φ = a (for air) and φ = b (for water-air mixture) yields the volumetric continuity equation which can be formulated as an implicit equation for pressure.

The governing equations are solved by a pressure-based method PIMPLE, which is a hybrid PISO/SIMPLE algorithm used to couple the pressure and velocity fields. Whilst the free surface is handled by a volume of fluid (VOF) method with bounded compression techniques.

3. Numerical simulation

To avoid simulating waves from the wavemaker through to breaking, generation of breaking waves can be performed by starting from an initial deformed free surface. With a suitable initial free surface shape for the numerical simulation, different types of wave impact on the wall can be easily generated (Scolan *et al.* [9]). Here we use a hyperbolic tangent shape to define the initial free surface:

$$y = h + A\tanh\big(R(x - L/2)\big), \quad 0 < x < L \tag{3}$$

where L is the length of the wave tank, h is the mean water depth, A is the amplitude of the mode and R is the parameter controls the slope of the difference in height. The shape is defined in a coordinate system where the origin is located at the bottom left corner. By varying the parameters, a large range of wave shapes can be generated to simulate different types of wave impact on the vertical wall.

There are many different classifications being used for wave impact. According to Bullock *et al.* [2], there are four distinct types of wave impacts, where the impact type changes with decreasing distance between the breaking point and the wall:

(a): the aerated impact, where the wave has broken in front and hits the wall with an aerated water mass;
(b): the air pocket impact, where the wave crest hits the wall with enclosing a thin air bubble;
(c): the flip through impact, where the wave crest hits the wall and runs up without trapping air bubble;
(d): the slosh impact, where the run up of the wave is higher than the wave crest, so that the wave crest hits the water layer instead of the wall.

We focus on air pocket and flip through impact in this investigation for the maximum impact pressure on the vertical wall. By setting constant parameters L = 2m, A = 0.16m and R = 5, and varying the mean water depth h from 0.22m to 0.26m, several cases of wave impact on a vertical wall are numerically simulated. The height of the numerical domain is chosen as 0.6m, which is much higher than the height of the initial free surface, to leave enough space for the air flow and wave impact to be fully developed.

For a mean water depth of 0.22m, with wave overturning and breaking on the vertical wall, the wave crest hits the wall and encloses a large air-pocket. With increasing the mean water depth, the size of the entrapped air-pocket decreases, until it vanishes. After that, the wave impact type changes from air-pocket impact to flip through impact, where the wave crest hits the wall and runs up without trapping air bubble. These can be seen clearly in Fig. 1, for h = 0.22m and 0.24m, the wave impacts on the wall with entrapped air bubble (air-pocket impact), while for h = 0.25m and 0.26m, the wave impacts on the wall without trapping air bubble (flip through impact).

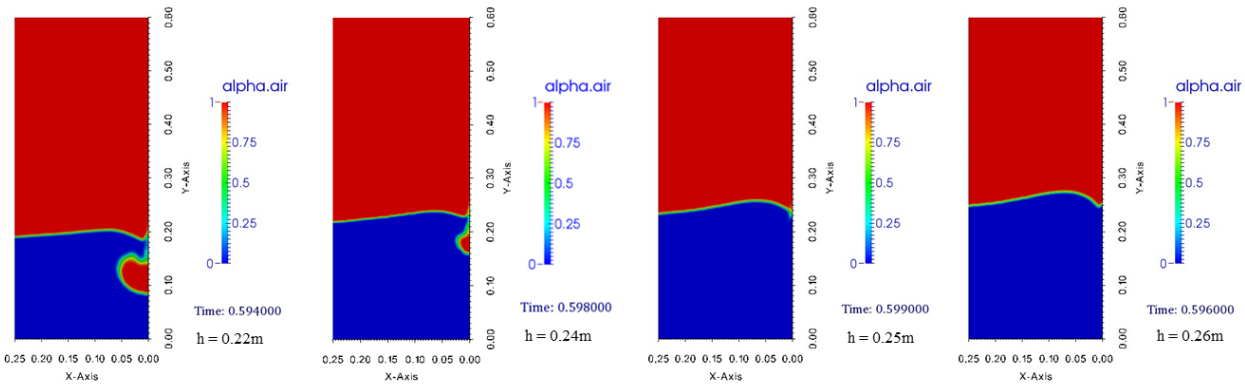

(a) air-pocket impact (b) flip through impact

Fig. 1. The free surface profiles at the time of peak impact for different initial water depths.

Fig. 2 shows the pressure distribution at the time of peak impact for different initial water depths relative to Fig. 1. The maximum pressure is located at the jet impact area. For an air-pocket impact, the pressure inside the air bubble is very high, and smaller air pockets tend to lead to higher pressures. For example, the air-pocket size for h = 0.24m is smaller than that for h = 0.22m, but the maximum pressure for h = 0.24m is 30kPa, which is much higher than 18kPa for h = 0.22m (Fig. 2 (a) and (b)). The flip through impact has a rather smaller impact area and generates a higher impact pressure (Fig. 2 (c) and (d)). For h = 0.25m, the maximum impact pressure reaches 51kPa, which is much higher than that of air-pocket impact.

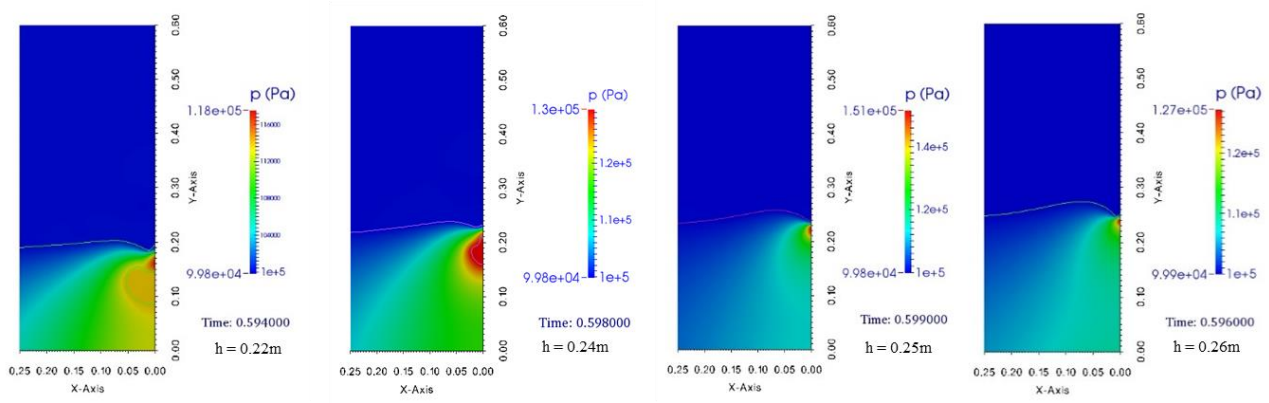

(a) air-pocket impact (b) flip through impact

Fig. 2. The pressure distributions at the time of peak impact for different initial water depths.

For the air-pocket impact, the entrapped air bubble is compressed horizontally against the wall by water pushing behind, and vertically by the trough run-up, which leads to oscillations of the air pocket (Bullock *et al.* [2]). The pressure on the wall will oscillate after the crest impact, associated with the compression and expansion of the air pocket. These phenomena can be seen clearly in Fig. 3 (a), the pressure on the wall oscillates after the peak impact where the measured points are located inside and below the air pocket. For the flip through impact, the pressure on the wall reaches to a sharp peak pressure when the wave crest hits the wall, and then damps very quickly with no pressure oscillation as shown in Fig. 3 (b). The duration of the high pressure impact is very small, less than 1ms.

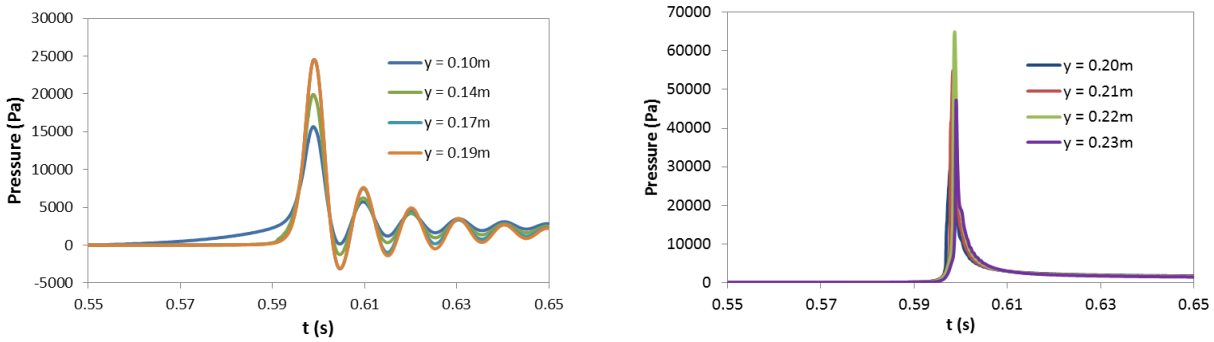

(a) air-pocket impact as h = 0.24 m (b) flip through impact as h = 0.25 m

Fig. 3. Time histories of impact pressure on the wall at different locations.

Fig. 4 shows the dimensionless pressure distributions along the wall for different initial water depths. It can be seen that the air-pocket impact causes a round peak pressure, which causes a larger impact area on the wall. The impact pressure for the small air pocket is larger than that for the big air pocket. The flip through impact exhibits a single sharp peak pressure, which indicates the larger impact pressure is not only related to smaller durations, but also to smaller impact areas. The largest pressure is created by flip through impact, for h = 0.25m, with the maximum dimensionless impact pressure reaching $p/\rho g h_o$=26. The mean water depth is also sensitive to the impact pressure. For ~1cm of difference in the mean water depth, the maximum impact pressure on the wall is reduced about 50%.

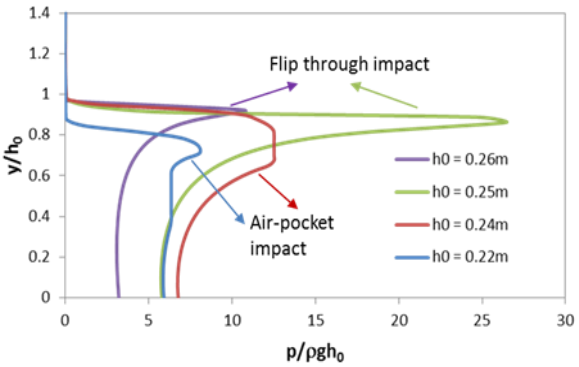

Fig. 4. Pressure along the wall at the moment of maximum impact pressure.

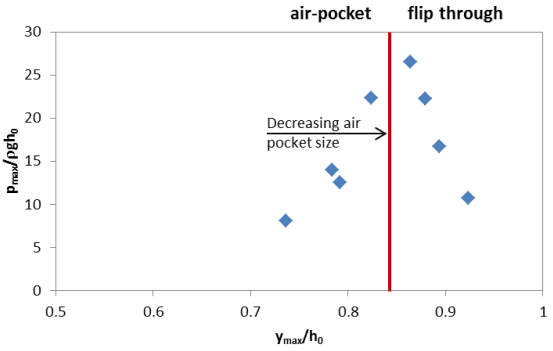

Fig. 5. Variation of dimensionless maximum impact pressures with impact locations

Fig. 5 shows the variation of dimensionless maximum impact pressures with impact locations. For the conditions of our predefined initial free surface, with increasing the mean water depth from mean water depth h = 0.22m to h = 0.26m, the wave impact point also occurs higher on the wall, whilst the trapped air pocket size decreases until it vanishes, corresponding maximum impact pressure reaches its peak value, and the impact type changes from air-pocket impact to flip through impact. After that, the maximum impact pressure will be reduced with increasing the mean depth, although impact location still grows higher

4. Conclusion

An open source compressible multiphase flow solver *twoPhaseEulerFoam* has been successfully used to simulate air-pocket and flip through wave impact on a vertical wall. The results show that the variability of the impact pressure is very large. The air pocket impact causes a round peak which happens at the location of the jet impact, whilst the flip through impacts exhibit a single sharp peak at the location where the wave crest and wave trough meet. The pressure oscillation inside the trapped air pocket has been recorded while the flip through impact does not generate pressure oscillation after the wave crest hits the wall.

Acknowledgements

This research was supported by the United Kingdom EPSRC Project: FROTH (Fundamentals and Reliability of Offshore Structure Hydrodynamics), under grant Ref: EP/J012777/1.

References

[1] Hattori M, Arami A & Yui T (1994) Wave impact pressure on vertical walls under breaking waves of various types. *Coastal Engineering.* Vol 22, pp 79-114.

[2] Bullock G, Obhrai C, Peregrine D, Bredmose H (2007). Violent breaking wave impacts. Part 1: Results from large-scale regular wave tests on vertical and sloping walls. *Coastal Engineering.* Vol 54, pp 602–617

[3] Peregrine DH (1993). Water-wave impact on walls. *Annual Review of Fluid Mechanics*. Vol 35, pp 23-43.

[4] Lin P and Liu PL-F (1999). Free surface tracking methods and their applications to wave hydrodynamics, Vol. 5 of Advances in Coastal and Ocean Engineering, World Scientific, pp 213-240.

[5] Christensen ED, Walstra DJ and Emarat N (2002). Vertical variation of the flow across the surf zone, *Coastal Engineering*, Vol 45, pp169-198.

[6] Jacobsen NG, Fuhrman DR and Fredsøe J (2012), A wave generation toolbox for the open-source CFD library: OpenFoam. *International Journal for Numerical Methods in Fluids*, Vol 70, Issue 9, pp 1073–1088.

[7] Chen LF, Zang J, Hillis AJ, Morgan GCJ and Plummer AR (2014), Numerical investigation of wave-structure interaction using OpenFOAM, *Ocean Engineering*, Vol 88, pp91-109.

[8] Morgan, G. and Zang, J. *et al.* (2010), Using the rasInterFoam CFD model for wave transformation and coastal modeling. The 32nd international Conference on Coastal Enginering (ICCE 2010).

[9] Scolan Y-M (2010), Some aspects of the flip-through phenomenon: A numerical study based on the desingularized technique, *Journal of Fluids and Structures*, Vol 26, Issue 6, pp 918-95.